Available online at www.elixirpublishers.com (Elixir International Journal)

Computational Chemistry

Elixir Comp. Chem. 71 (2014) 24793-24802

ISSN: 2229-712X

Geometry and vibrational analysis of 2-amino thiazole - quantum chemical study

R.Karunathan[1], V.Kannappan[2] and V.Sathyanarayanamoorthi[1,*]

[1]Department of Physics, PSG College of Arts and Science, Coimbatore-641 014, India.

[2]Department of Chemistry, Presidency College, Chennai-600 005, India.

ARTICLE INFO

Article history:

Received: 27 April 2014;

Received in revised form:

25 May 2014;

Accepted: 6 June 2014;

Keywords

DFT,

Ab initio,

NBO.

ABSTRACT

The Fourier transform infrared (FT-IR) and FT-Raman of 2-Amino thiazole (2-AT) have been recorded and analyzed. The equilibrium geometry, bonding features and harmonic vibrational frequencies have been investigated with the help of ab initio and density functional theory (DFT) methods. The assignments of the vibrational spectra have been carried out. The optimized geometric bond lengths and bond angles obtained by computation show good agreement with experimental data of the relative compound. The computed parameters also show good agreement with experimental data. The calculated HOMO and LUMO energies also show that charge transfer occurs within the molecule. Stability of the molecule arising from hyperconjugative interactions, charge delocalization have been analyzed using natural bond orbital (NBO) analysis. The results show that charge in electron density (ED) in the σ* and π* antibonding orbital and second order delocalization energies E(2) confirms the occurrence of intramolecular charge transfer (ICT) within the molecule. Finally the calculations results were applied to simulated infrared and Raman spectra of the title compound which show good agreement with observed spectra.

Introduction

2-Aminothiazole (abbreviated 2AT) is regarded as a privileged structure motif in medicinal chemistry due to its presence in the numerous pharmaceuticals [1, 2] and agrochemicals [3]. The decoration of 2-aminothiazole is, therefore, of great current interests. In particular, the incorporation of fluoroalkyl groups into 2AT represents an attractive strategy in this regard (Scheme 1) [4-6], since it is well-known that fluorination of less active precursors often leads to potent drugs with enhanced bioavailability, reduced toxicity or improved affinity for the target receptor [7,8]. Pharmacologically, 2-aminothiazoles are among the most important classes of organic compounds. These compounds possess versatile type of biological activities; some of these are well known for their anti-inflammatory activities such as Fentiazac1 and Meloxicam, 2 while compounds like Nizatidine possess anti-ulcer activity. In recent years, among the computational methods calculating the electronic structure of molecular systems, DFT has been favorite one due to its great accuracy in reproducing the experimental values of in molecule geometry, vibrational frequencies, atomic charges, dipole moment, thermodynamical properties, etc. [10]. Related to this phenomenon, we wish to present here the spectroscopic properties and electronic structure of 2-AT.

Methodology

Experimental Details

The compound under investigation namely 2-AT is purchased from M/S Aldrich Chemicals, (USA) with spectroscopic grade and it is used as such without any further purification. The F T-IR spectrum of the compound was recorded in Perkin–Elmer Spectrometer in the range of 4000-100 cm-1 using KBr pellet technique. The spectral resolution is 0.1cm^{-1}. The FT-Raman spectrum of the compound was recorded in the BRUK ER RFS 27 and Stand alone F T-Raman Spectrometer in the frequency range 50-4000 cm-1 . The Laser source is Nd:YAG laser source operating at 1064 nm line with 200 mW power. The spectra were recorded with scanning speed of 20cm^{-1} . The frequencies of all sharp bands are accurate to ±1 cm^{-1}.

Computational Details

The molecular geometry optimization and vibrational frequency calculations were carried out 2-Amino-6-nitro benzothiazole, with GAUSSIAN 09W software package [9] HF functional [10] combined with standard 6-311++G(d,p) basis set (referred to as “large” basis) and the density functional method used is B3LYP i.e. Becke’s three-parameter hybrid functional with the Lee–Yang–Parr correlation functional method with 6-311++G(d,p).

Results and discussion

Molecular Geometry

The labeling of atoms in 2-AT is given in Fig. 1. The structural parameters obtained by ab initio HF/6-311++G (d, p) levels basis set are compared to density functional theory B3LYP/6-311++G (d, p) levels basis set theory data for 2-Amino thiazole [11] reported in Table 1. The comparative graphs of bond lengths and bond angles of the title molecule presented in Figs. 2 and 3 respectively. From the theoretical values, it is found that most of the optimized bond lengths are slightly larger than the experimental values [12], due to that the theoretical calculations belong to isolated molecules in gaseous phase and the experimental results belong to molecules in solid state. Comparing bond angles and lengths of B3LYP with those of HF, as a whole the formers are bigger than later and the B3LYP calculated values correlates well compared with the experimental data. Although the differences, calculated geometrical parameters represent a good approximation and they are the bases for the calculating other parameters, such as vibrational frequencies and thermodynamics properties. From

Tele:

E-mail addresses: sathyanarayanamoorthi@yahoo.co.in

the data shown in Table 1, it is seen that both HF and DFT (B3LYP/6-311++G (d, p)) levels of theory in general estimate same values of some bond lengths and bond angles.

The phenyl ring appears to be a little distorted from its regular symmetry as the computed bond lengths: S_1-C_2 >S_1-C_4 > S_1-C_5> C_2-N_3> C_2-N_6 > N_3-C_4 > C_4-C_5. The irregular symmetry of the Phenyl ring is also evident from the decrease in value of the bond angles at the substitution position as in table 1. The ring twisting influences the delocalization of the π-electrons and can explain the charges of optical as well as the electronic properties of the substituent's [13]. Although theoretical results are not exactly close to the experimental values for the compounds, they generally accept that bond lengths and bond angles depend on the method and the basis set used in the calculations and they could be used as foundation to calculate the molecular properties for the compounds.

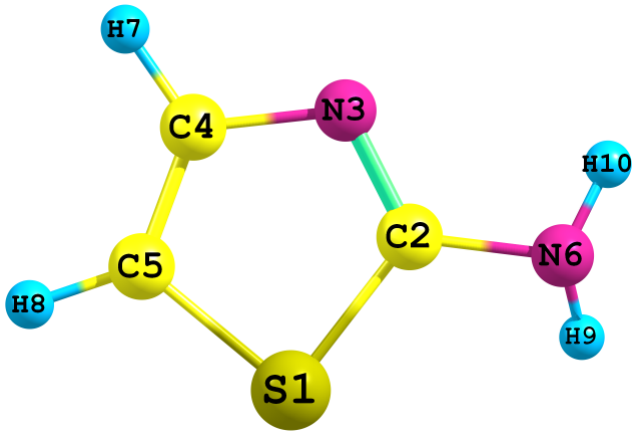

Fig.1 Optimized structure of 2-Amino thiazole

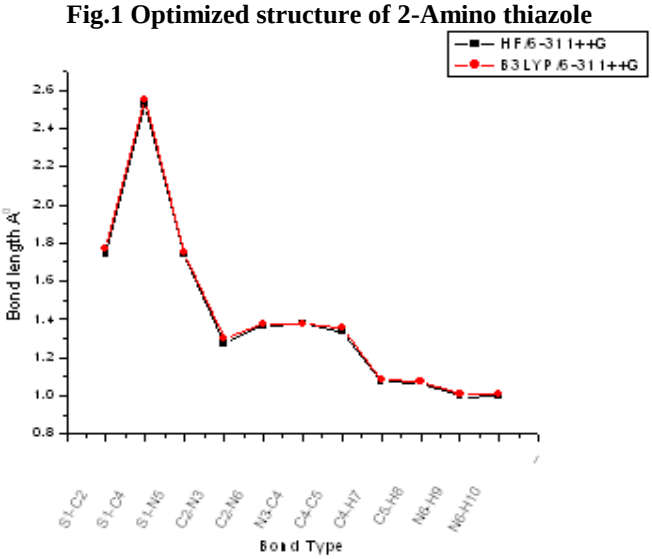

Fig 2.Bond length difference between theoretical (HF and DFT) approaches

Thermodynamic properties

The values of some thermodynamic parameters (such as zeropoint vibrational energy, thermal energy, specific heat capacity, rotational constants, entropy, etc.) of 2-AT at 298.15 K in ground state are listed in Table 2. The variation in Zero-Point Vibrational Energies (ZPVEs) seems to be significant. The ZPVE is much lower by the DFT/B3LYP method than by the HF method. The biggest value of ZPVE of 2-AT are 45.056kcl/mol obtained at HF/6-311++G(d,p) whereas the smallest values are 42.292 kcal/mol obtained at B3LYP/6-311++G(d,p). Dipole moment reflects the molecular charge distribution and is given as a vector in three dimensions. Therefore, it can be used as descriptor to depict the charge movement across the molecule. Direction of the dipole moment vector in a molecule depends on the centers of positive and negative charges. Dipole moments are strictly determined for neutral molecules. For charged systems, its value depends on the choice of origin and molecular orientation. As a result of HF and DFT (B3LYP) calculations the highest dipole moment was observed for B3LYP/6-311G++(d,p) whereas the smallest one was observed for HF/6-311++G(d,p) in each molecule.

On the basis of vibrational analysis, the statically thermodynamic functions: heat capacity (C), entropy (S), and enthalpy changes (ΔH) for the title molecule were obtained from the theoretical harmonic frequencies and listed in Table 6. From the Table 6, it can be observed that these thermodynamic functions are increasing with temperature ranging from 100 to 600 K due to the fact that the molecular vibrational intensities increase with temperature [14].

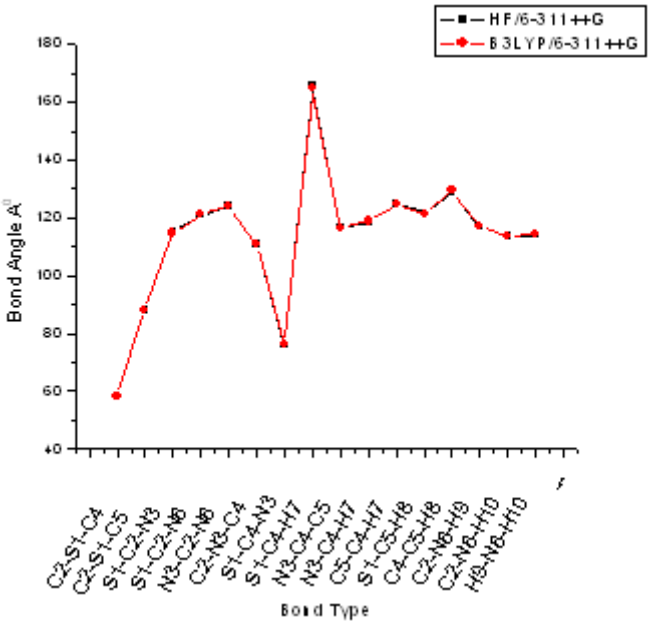

Fig 3.Bond Angle difference between theoretical (HF and DFT) approaches

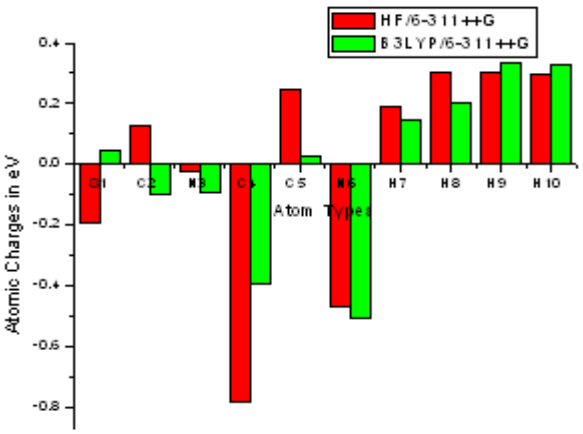

Fig. 4. Mullikan's Atomic charges between theoretical (HF and DFT) approaches

Mulliken atomic charges

Mulliken atomic charge calculation has an important role in the application of quantum chemical calculation to molecular system because of atomic charges effect dipole moment, molecular polarizability, electronic structure and more a lot of properties of molecular systems. The calculated Mulliken charge values are listed in Table 3. The charge changes with basis set presumably occur due to polarization.

Table 1 Optimized geometrical parameters of 2 Amino thiazole, bond length (A),bond angles (◦)

Parameters	HF/6-311++G	B3LYP/6-311G
Bond length		
S_1-C_2	1.7445	1.7675
S_1-C_4	2.5205	2.5476
S_1-N_5	1.7442	1.7497
C_2-N_3	1.2756	1.2988
C_2-N_6	1.3688	1.3768
N_3-C_4	1.3794	1.3788
C_4-C_5	1.3355	1.3565
C_4-H_7	1.0725	1.0818
C_5-H_8	1.0692	1.0779
N_6-H_9	0.9946	1.0086
N_6-H_{10}	0.9964	1.0108
Bond angle		
C_2-S_1-C_4	58.2821	58.1331
C_2-S_1-C_5	88.3167	88.2498
S_1-C_2-N_3	115.1371	114.7305
S_1-C_2-N_6	120.8936	121.1556
N_3-C_2-N_6	123.9082	124.0072
C_2-N_3-C_4	110.6886	110.8001
S_1-C_4-N_3	75.8922	76.3361
S_1-C_4-H_7	165.5753	164.841
N_3-C_4-C_5	116.7131	116.6657
N_3-C_4-H_7	118.5325	118.8227
C_5-C_4-H_7	124.7531	124.5088
S_1-C_5-H_8	121.7448	121.0068
C_4-C_5-H_8	129.1141	129.4435
C_2-N_6-H_9	116.8864	117.3662
C_2-N_6-H_{10}	113.418	113.4294
H_9-N_6-H_{10}	114.0768	114.1436

Table 2, The calculated thermo dynamical parameter of 2-amino thiazole

Basis Set	HF/6-311++G (d, p)	B3LYP/6-311++G (d, p)
Zero point energy (Kcal/Mol)	45.056	42.292
Rotational constant	5.773	5.773
Rotational temperature	0.277	0.277
Energy (E)		
Translational	0.889	0.889
Rotational	0.889	0.889
Vibrational	46.381	43.985
Total	48.159	45.763
Specific heat (C_v)		
Translational	2.981	2.981
Rotational	2.981	2.981
Vibrational	13.022	15.283
Total	18.983	21.245
Entropy(S)		
Translational	39.718	39.718
Rotational	26.705	26.705
Vibrational	6.190	8.180
Total	72.614	74.604
Dipole moment	0.88	1.03

Table 3. Mulliken atomic charges of 2-Amino thiazole

Atoms	HF/6-311++G(d,p)	B3LYP/6-311++G(d,p)
S_1	-0.196	0.045
C_2	0.130	-0.096
N_3	-0.021	-0.093
C_4	-0.782	-0.394
C_5	0.248	0.029
N_6	-0.468	-0.506
H_7	0.188	0.145
H_8	0.301	0.202
H_9	0.301	0.336
H_{10}	0.297	0.330

Table 4. Experimental and calculated absorption wavelength (nm), excitation energies E (eV) and oscillator strengths (f) of 2-amino thiazole

Exp Ethanol		TD-HF/6-311++G (d,p) Ethanol			TD-HF/6-311++G (d,p) Gas phase		
λ (mn)	(f)	λ (mn)	(f)	E (eV)	λ (mn)	(f)	E (eV)
240.00	4.00	224.31	0.1469	5.5273 eV	223.75	0.1075	5.5412 eV
201.00	4.00	199.9	0.0032	6.2025 eV	204.01	0.0058	6.0772eV
217.00	1.63	196.91	0.0215	6.2963 eV	199.93	0.0195	6.2012eV

Table 5. Comparison of the experimental (FT-IR and FT-Raman) and theoretical harmonic wave numbers (cm^{-1}) of 2 Amino thiazole calculated by HF, B3LYP with 6-311++G (d, p) basis set.

Modes No	Experimental		6-311++G	B3LYP 6-311++G	Assignment
	IR	Raman			
1.			322	258	C- NH_2 Out of plane bending
2.	402	397	388	351	C- NH_2 in plane bending
3.	471		477	380	NH_2 twisting
4.	513	566	556	380	C-H Out of plane bending
5.			582	484	Ring stretching
6.			613	502	NH_2 wagging
7.	643		631	548	C-S Stretching
8.	693	676	646	651	C-H Out of plane bending
9.	758	759	774	692	C-H Out of plane bending
10.			807	753	C-H Out of plane bending
11.	882	883	826	882	Ring stretching
12.			985	988	C-H in plane bending
13.	1028	1031	1083	972	NH_2 Rocking
14.		1073	1121	1101	C-H in plane bending
15.	1200	1205	1177	1212	C-N Stretching
16.	1359	1277	1320	1254	C=C Stretching
17.	1384	1498	1350	1422	N-H in plane bending
18.	1522	1642	1542	1648	N-H_2 in plane bending
19.	1761		1778	1736	C=N Stretching
20.			1809	1809	N-H wagging
21.	3136	3066	3089	3041	C-H Stretching
22.			3161	3117	C-H Stretching
23.	3290	3121	3179	3144	N-H Asymmetric Stretching
24.	3409		3307	3275	N-H symmetric Stretching

Table 6. Comparative values of IR and Raman intensities between HF/ 6-311G++ (d, p) and B3LYP/ 6-311G++(d, p) of 2-amino thiazole.

HF/6-311++G (d,p)		B3LYP/6-311++G (d,p)	
IR Intensity	Raman intensity	IR Intensity	Raman intensity
28.940	11.554	84.763	19.912
8.125	1.978	14.411	3.299
241.73	6.329	150.496	9.222
16.107	3.508	13.036	2.311
9.598	15.202	30.635	2.622
4.878	4.991	2.895	16.096
25.350	4.533	17.853	7.537
11.792	15.364	10.386	19.378
5.845	1.814	9.845	6.320
46.954	0.377	33.825	0.390
1.823	1.197	1.384	1.566
107.72	2.799	122.806	3.610
97.483	2.490	9.261	0.735
6.680	1.135	77.489	6.137
3.506	13.553	13.501	4.008
33.271	17.908	10.366	4.418
3.010	0.223	9.435	13.064
14.902	8.686	3.509	9.862
151.073	2.505	34.991	5.305
32.851	2.103	120.689	3.123
65.225	8.642	57.419	10.399
49.015	5.768	33.448	8.661
71.359	9.713	52.553	14.067
91.111	2.764	66.521	3.437

Table 7. Second order perturbation theory analysis of Fock matrix in NBO basis for 2-Amino Thiazole

Donor (i)	Type	ED/e	Acceptor (j)	Type	ED/e	$E^{(2)}$ (kJ mol−1)[a]	E(j) - E(i)[b] (a. u.)	F (i,j)[c] (a. u.)
S_1-C_2	σ	1.97743	S_1-C_5	σ*	1.97159	1.48	1.12	0.036
			N_3-C_4	σ*	1.96918	0.61	1.40	0.026
			C_4-H_7	σ*	1.98306	5.65	1.46	0.081
			C_5-H_8	σ*	1.98595	1.71	1.42	0.044
			N_6-H_{10}	σ*	1.98766	1.14	1.39	0.036
S_1-C_5	σ	1.97159	S_1 - C_2	σ*	0.07880	1.59	1.06	0.037
			C_2 - N_3	σ*	0.02612	0.67	1.64	0.030
			C_2 - N_6	σ*	0.03246	2.16	1.32	0.048
			N_3 - C_4	σ*	0.01661	1.73	1.34	0.043
			C_4 - H_7	σ*	0.02757	12.24	1.40	0.117
C_2 - N_3	σ	1.99080	C_2 - N_6	σ*	0.03246	1.73	1.81	0.050
			N_3 - C_4	σ*	0.01661	1.74	1.83	0.050
			C_4 - C_5	σ*	0.01666	1.21	2.01	0.044
			C_4 - H_7	σ*	0.02757	1.55	1.89	0.049
C_2 - N_3	π	1.90603	C_4 - C_5	π*	0.14651	30.49	0.62	0.124
			N_6 - H_9	σ*	0.00519	2.49	1.07	0.047
			N_6 - H_{10}	σ*	0.00667	2.37	1.07	0.046
C_2 - N_6	σ	1.99267	C_2 - N_3	σ*	0.03246	1.14	1.93	0.042
			N_3 - C_4	σ*	0.01661	3.33	1.63	0.066
N_3 - C_4	σ	1.96918	S_1 - C_2	σ*	0.07880	1.46	1.27	0.039
			C_2 - N_3	σ*	0.02612	1.21	1.85	0.042
			C_2 - N_6	σ*	0.03246	16.01	1.53	0.140
			C_4 - C_5	σ*	0.01666	1.70	1.73	0.049
			C_5 - H_8	σ*	0.00698	1.32	1.57	0.041
C_4 - C_5	σ	1.99011	S_1 - C_2	σ*	0.01583	1.02	1.30	0.033
			C_2 - N_6	σ*	0.03246	0.83	1.56	0.032
			N_3 - C_4	σ*	0.01661	0.63	1.58	0.028
			C_4 - H_7	σ*	0.02757	1.12	1.64	0.038
			C_5 - H_8	σ*	0.00698	1.69	1.61	0.047
C_4 - C_5	π	1.94493	C_2 - N_3	π*	0.20472	11.22	0.56	0.074
C_4 - H_7	σ	1.98306	S_1 - C_5	σ*	0.01583	4.25	1.02	0.059
			C_2 - N_3	σ*	0.02612	2.41	1.60	0.055
C_5 - H_8	σ	1.98595	N_3 - C_4	σ*	0.01661	6.26	1.39	0.083
			C_4 - C_5	σ*	0.01666	3.63	1.57	0.068
N_6 - H_9	σ	1.98501	C_2 - N_3	σ*	0.02612	1.13	1.77	0.040
N_6 - H_{10}	σ	1.98766	S_1 - C_2	σ*	0.07880	2.87	1.18	0.053
			C_2 - N_3	π*	0.20472	1.98	1.03	0.042
C_2 - N_3	π*	0.20472	C_2 - N_6	σ*	0.03246	0.64	0.42	0.042
			N_6 - H_9	σ*	0.00519	1.21	0.43	0.063
			N_6 - H_{10}	σ*	0.00667	1.23	0.43	0.063
C4 - C5	π*	0.14651	C_2 - N_3	π*	0.20472	73.90	0.02	0.077

Table 8. Second-order perturbation energies E (2) (donor → acceptor) for 2-Amino Thiazole

Donor (i)	Acceptor (j)	E (2) (kJ mol−1) [a]	E (j) – E (i) [b] (a. u.)	F (I,j) [c] (a. u.)
Within unit 1				
LP (1) S1	σ*C2-N3	2.60	1.72	0.060
LP (1) S1	σ*C5-H8	0.71	1.44	0.029
LP (2) S1	π*C2-N3	35.41	0.52	0.121
LP (2) S1	π*C4-C5	13.39	0.50	0.074
LP (1) N3	σ*S1-C2	17.57	0.91	0.113
LP (1) N3	σ*C2-N6	2.64	1.17	0.050
LP (1) N3	σ*C4-C5	9.23	1.38	0.102
LP (1) N3	σ*C4-H7	3.47	1.25	0.060
LP (1) N6	σ*S1-C2	13.42	0.74	0.089
LP (1) N6	σ*S1-C5	0.51	0.74	0.018
LP (1) N6	σ*C2-N3	11.53	1.32	0.111
LP (1) N6	σ*C2-N3	4.51	0.58	0.047

For example, the charge of N (6) atom is -0.468176 for HF/6-311++G (d, p) and -0.506083 B3LYP/6-311++G (d,p). The charge distribution of amine group is increasing trend in HF and B3LYP methods. The charge of H_7, H_8, H_9, and H_{10} is positive in both HF and DFT diffuse functions. Considering the all methods and basis sets used in the atomic charge calculation, the carbon atoms exhibit a substational negative charge, which are donor atoms. Hydrogen atom exhibits a positive charge, which is an acceptor atom. The Mulliken charge distribution of 2AT is increasing trend in B3LYP as Compared to HF methods. The Graphical representation is depicted in Figure 4.

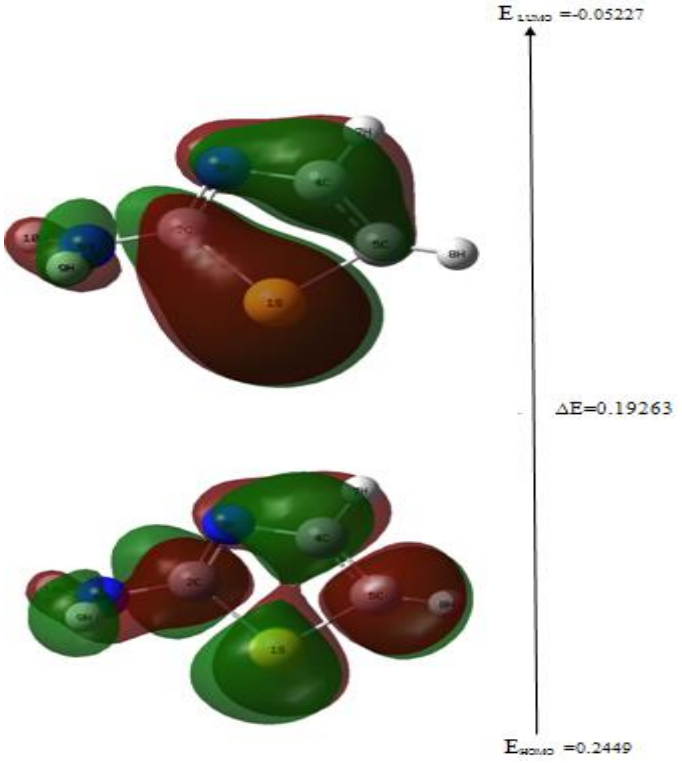

Fig. 5. The molecular orbitals and energies for the HOMO and LUMO of the title compound

Frontier molecular orbitals (FMOs)

The highest occupied molecular orbital's (HOMOs) and the lowest-lying unoccupied molecular orbitals (LUMOs) are named as frontier molecular orbital's (FMOs). The FMOs play an important role in the optical and electric properties, as well as in quantum chemistry and UV–vis spectra [15]. The HOMO represents the ability to donate an electron, LUMO as an electron acceptor represents the ability to obtain an electron. The energy gap between HOMO and LUMO determines the kinetic stability, chemical reactivity and optical polarizability and chemical hardness–softness of a molecule [16,17].

In order to evaluate the energetic behavior of the title compound, we carried out calculations in vacuo and in organic solvent (ethanol)illustrated in Fig 5 and table 4. The energies of important molecular orbitals of 2AT: the highest occupied MOs (HOMO), the lowest unoccupied MOs (LUMO) were calculated using HF/6-311++G(d,p).The HOMO and LUMO values -0.2449,-0.05227 respectively. The 3D plots of the HOMO, LUMO orbitals computed at theHF/6-311G++(d,p) level for 2-AT molecule are illustrated in Fig.6. The positive phase is red and the negative one is green. It is clear from the figure that, while the HOMO is localized on almost the whole molecule, LUMO is localized on the phenyl ring. Both the HOMOs and the LUMOs are mostly π anti-bonding type orbital's. The calculated energy value of HOMO is -0.2449a.u. And LUMO is -0.05227 a.u. in, respectively. The value of energy separation between the HOMO and the LUMO is 0.19263 respectively. The energy energy separation between the HOMO and the LUMO is 0.19263 respectively. The energy gap of HOMO–LUMO explains the eventual charge transfer interaction within the molecule, which influences the biological activity.

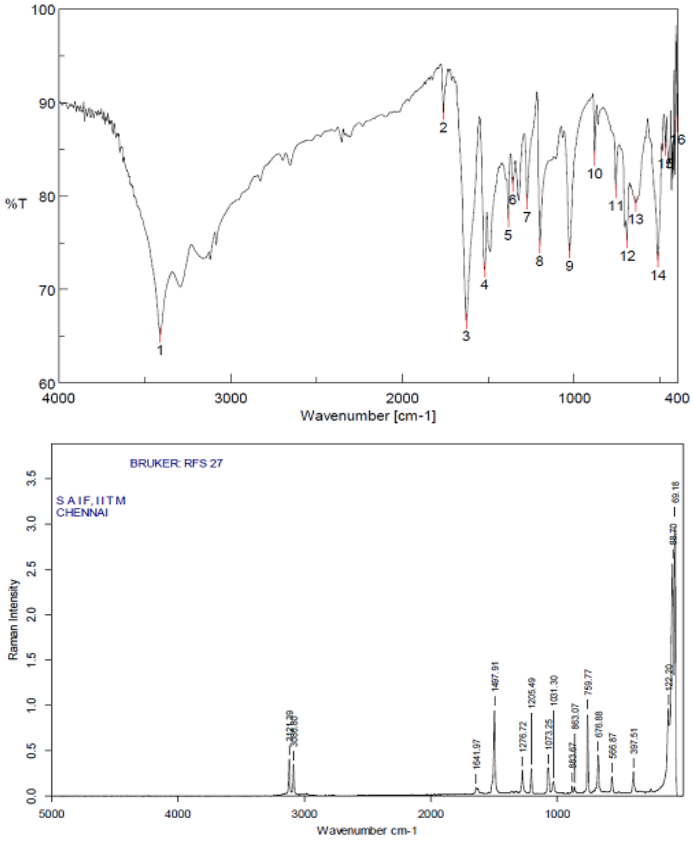

Fig.6. Experimental FT-IR and FT-Raman Spectrum of 2-amino thiazole

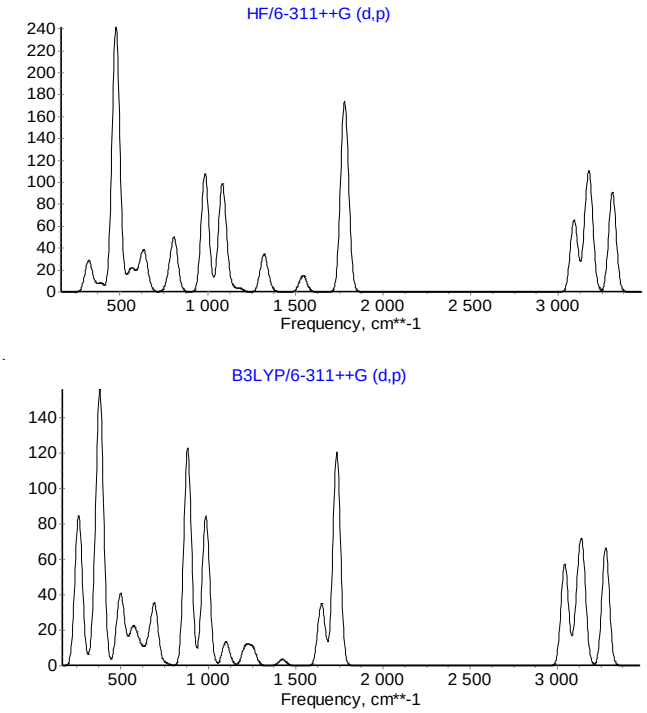

Fig.7. Theoretical FT-IR Spectrum of 2-amino thiazole

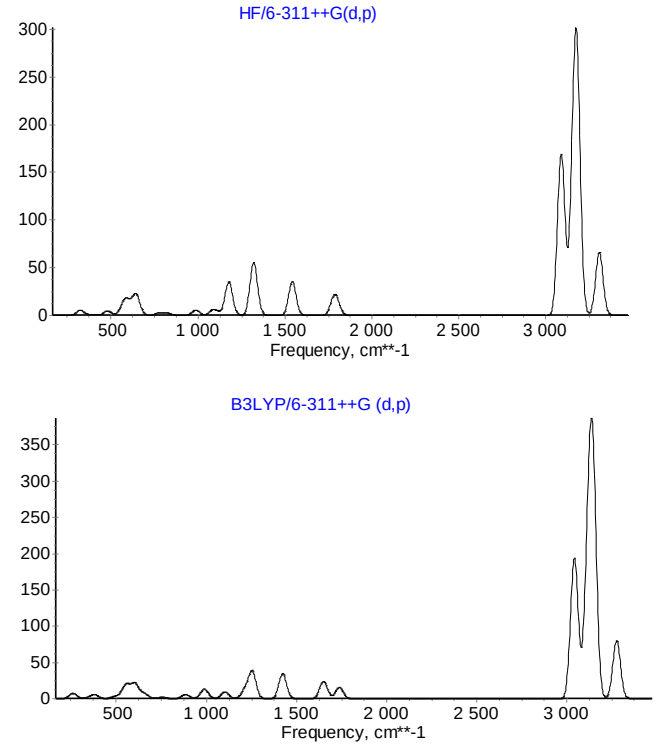

Fig.8 Theoretical FT-Raman Spectrum of 2-amino thiazole

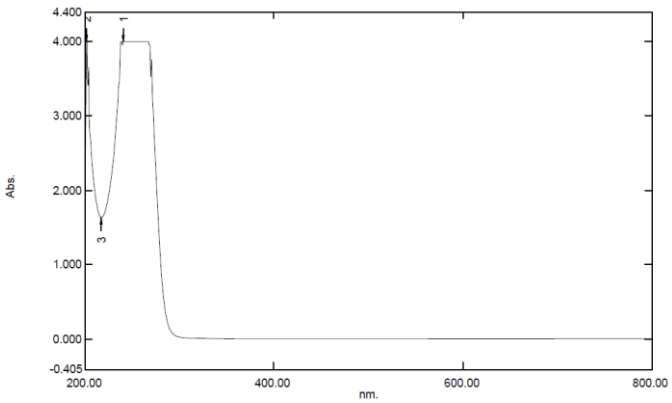

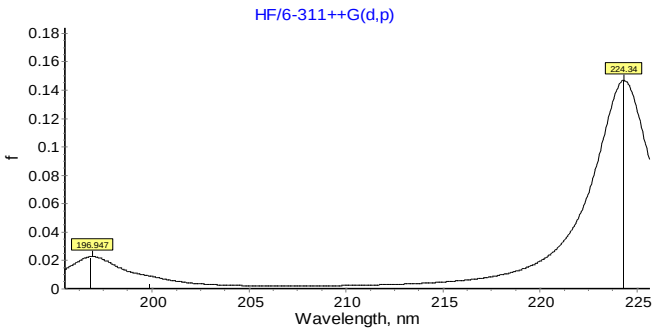

Fig. 9 Experimental and theoretical UV–vis spectrum in ethanol for the title molecule calculated with the TD-HF/6-311++G (d, p) method

Comparative vibrational frequency analysis

Many numbers of potentially active observable fundamentals of a Non-linear molecule which contain N atom is equal to (3N-6), apart from three dimensional and three rotational degrees of freedom. Hence, 2-AT molecule, which has 10 atoms with 24 normal modes of vibrations. All vibrations are active both in Raman and infrared absorption. The detailed vibrational assignment of the experimental wave numbers is based on normal mode analyses and a comparison with theoretically calculated wave numbers by B3LYP and HF methods. The observed and simulated infrared and Raman spectra of 2-amino thiazole is shown in Figs. 7,8 and 9, respectively. The observed and scaled theoretical frequencies using HF and DFT (B3LYP) with 6-311++G(d,p) basis sets with vibrational assignments are listed in Table 5.the comparative graphs are shown in Fig.10.

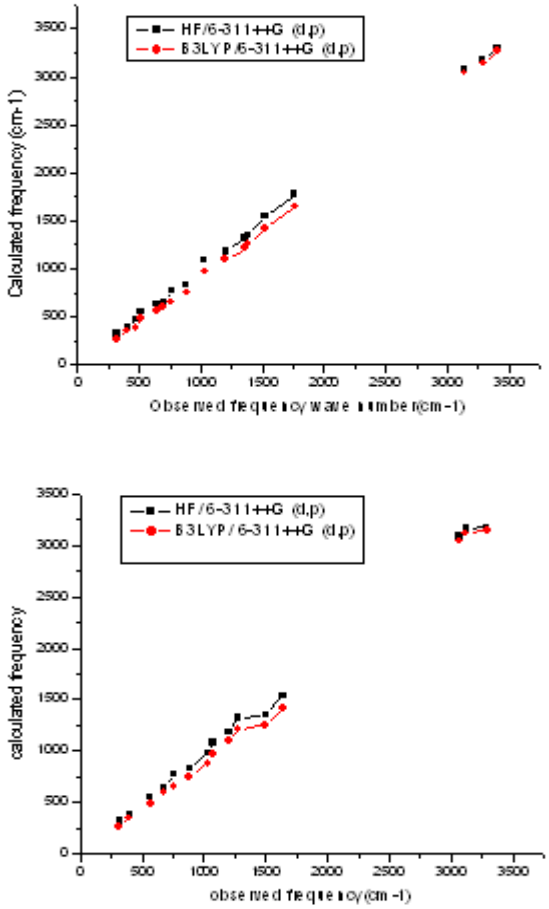

Fig.10. Comparative graph of experimental FT-IR and FT-Raman and calculated frequency

Vibrational analysis

C-H vibrations

The range 3100-3000 cm^{-1} which is the characteristic region for ready to identification of C-H Stretching vibration [18-20]. The bands captured at 3088, 3162 cm^{-1} in FTIR and 3066 cm^{-1} in the FT-Raman spectra for 2-AT have been assigned to C-H Stretching vibration.

The C-H in plane bending usually occurred in the region 1300-1000 cm^{-1} [21].here the C-H in plane bending vibration of the titled compound are observed at 990 to 1200 cm^{-1} in FT-IR and 1073 in FT-Raman. Theoretically calculated vibrations by HF and B3LYP/6-311++G (d, p) level methods good agreement with the experimentally recorded data.

The C-H out of plane bending vibrations are appeared within the region 900-675 cm^{-1} [22-24]. In this present title molecule the C-H out of plane bending vibrations captured at the region 807,774,646 cm^{-1}in FT-IR and 676,780 cm^{-1} FT-Raman are assigned to C-H out of plane bending. The calculated HF/6-311++G (d,p)frequencies were well matched with B3LYP/6-311++G(d,p) frequencies results. These out of plane bending vibrational frequencies are found to be well within their characteristic region.

C=C and ring vibrations

Generally C= C stretching vibrations occurred in the region of 1430–1650 cm^{-1} [26, 27]. Accordingly, In the present study, the C=C stretching vibrations of 2Amino thiazole are observed at 1356 cm^{-1} in FT-IR and 1276 cm^{-1} in FT-Raman, both this two results are well matched with theoretical calculation frequencies results. The ring stretching vibrations in FT-IR and FT-Raman are assigned to 883,884 cm^{-1} respectively. The calculated HF/6-311++G (d,p)frequencies were coincide with B3LYP/6-311++G(d, p) (DFT)frequencies results.

C-S vibration

In general, the assignment of the band due to C–S stretching vibrations in different compounds is difficult. Which is mostly weak to medium bands due to C–S stretching vibration in the region 780–510 cm^{-1} [28]. The major weak FT-I R band observed at 644 cm^{-1} are assigned to this mode, since the FT-Raman spectra don't show any of the bands. Theoretically it is computed by HF/6-311+G (d,p) and B3LYP/6-311+G(d,p) methods at 632 and 548 cm^{-1} show good agreement with the experimental values.

Amino group vibrations

The C–N stretching frequency is a rather difficult task since there are problems determinations of these frequencies from other vibrations. The C–N stretching absorption in the region 1382–1266 cm^{-1} for aromatic amines [29-31]. In this study, the band at 1201cm^{-1} in FT-IR and 1205 cm^{-1} in FT-Raman spectrum is assigned to C–N stretching vibration. Theoretically it is predicted scale value at 1212 cm^{-1} (B3LYP) and 1178 cm^{-1} (HF) (mode No. 15) show excellent agreement with experimental data. The C=N band is observed at 1762 cm^{-1} in FT-IR spectrum.

N–H vibrations

Usually, the N–H stretching vibrations occur in the region3500–3300 cm^{-1}. The asymmetric $–NH_2$ stretching vibration appears from 3500 to 3420 cm^{-1} and the symmetric $–NH_2$ stretching is observed in the range 3420–3340 cm^{-1}. In this study, the NH_2 asymmetric stretches captured at 3410 cm^{-1} in FT-IR spectrum. It is good agreement with HF and B3LYP/6-311++G (d, p) calculated values. The in-plane NH_2 in-plane deformation vibrations occur in the short range 1650–1580 cm^{-1}region of the spectrum. Therefore, a very strong band is observed in FT-IR at1521 $cm^{-1}$and FT-Raman at 1641 $cm^{-1}$was assigned to in-plane deformation mode of the amino group. The amino in-plane bending rocking mode normally appears in the range 1150–900 cm^{-1} while the wagging bands between 850 and 500 cm^{-1}. Therefore, the bands at 619 and 470 $cm^{-1}$are attributed to the wagging and twisting modes of amino group, respectively.

The rocking mode was observed at 1027cm^{-1}in FT-IR and 1031 cm^{-1} in FT-Raman respectively. Following this frequencies are very good agreements with theoretical values, Hatree -fock frequencies are well matched with DFT results. These amino vibrations are also in good agreement with literature values of aniline [32], 4-aminoquinaldine [33] and 5-aminoquinoline [34].

Computed IR intensity and Raman intensity analysis

Computed vibrational spectral IR intensities and Raman activities of the 2AT molecule for corresponding wave numbers by HF and DFT (B3LYP) methods at 6-311++G(d,p) basis set have been collected in the Table 6. Comparison of IR intensities and Raman intensities calculated by HF and DFT (B3LYP) at 6-311++G (d,p) level with experimental values exposes the variation of IR intensities and Raman activities[Fig.11]. In most of the cases, the values of IR intensities by HF are found to be higher than B3LYP at 6-311++G(d,p) level whereas in the case of Raman intensities the effect is reversed.

NBO analysis

The natural bond orbital analysis provides an efficient method for studying intra- and inter-molecular bonding and interaction among bonds, and also provides a convenient basis for investigating charge transfer or conjugative interaction in molecular systems. Some electron donor orbital, acceptor orbital and the interacting stabilization energy resulting from the second-order micro disturbance theory are reported [35,36]. NBO analysis has been performed on the molecule at the HF/6-311++G(d,p) level in order to elucidate the intramolecular, rehybridization and delocalization of electron density within the molecule, which are presented in Tables 7 and 8.The result of interaction is a loss of occupancy from the concentration of electron NBO of the idealized Lewis structure into an empty non-Lewis orbital. For each donor (i) and acceptor (j), the stabilization energy E (2) associated with the delocalization i→j is estimated as

$$E(2) = -n_\sigma \frac{\langle \sigma | F | \sigma \rangle^2}{\varepsilon_\sigma^* - \varepsilon_\sigma} = -n_\sigma \frac{F_{ij}^2}{\Delta E}$$

Where

$\langle \sigma | F | \sigma \rangle^2$ or $F_{ij}^2$is the Fock matrix element i and j NBO orbital's, ε_σ^* and - ε_σ are the energies of σ and σ * NBOs and n_σ is the population of the donor σ orbital.

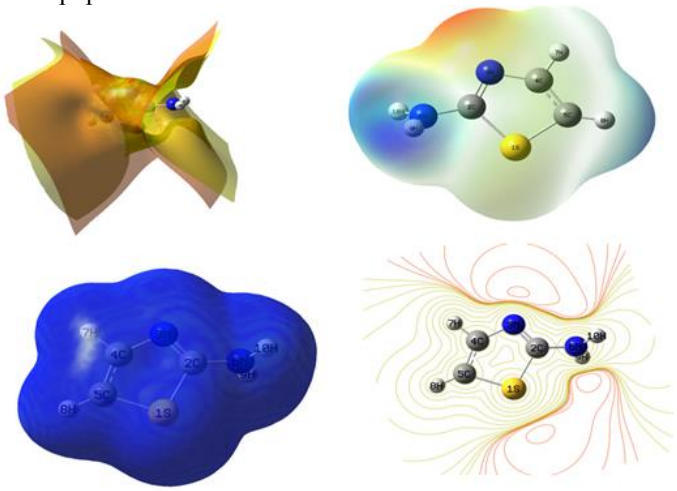

Figure 11. Electrostatic potential (ESP), The molecular electrostatic potential map (MEP),Total electron density (TED), Electrostatic potential contour map and for the title molecule

A large diversity of energy values was found. The stronger donor character is shown by the p-type lone pair of the nitrogen atoms. The most important interaction (n–σ*) energies, related to the resonance in the molecules, are electron donation from the LP(1)S atoms of the electron donating groups to the anti-bonding acceptor π*(C–N) of the phenyl ring ($LP(1)S_1 \rightarrow \pi^*(C_2–N_3)$ = 35.41kJ mol^{-1}. This larger energy shows the hyperconjugation between the electron donating groups and the phenyl ring. NBO analysis has been performed on the 2-AT at the HF/6-311++G (d,p) level in order to elucidate, the intramolecular, rehybridization and delocalization of electron density within the molecule. The intramolecular interaction are formed by the orbital overlap between bonding (C–C) and (C–C) anti-bond orbital which results intramolecular charge transfer (ICT) causing stabilization of the system. These interactions are observed as increase in electron density (ED) in C–C anti-bonding orbital that weakens the respective bonds. The strong intramolecular hyper conjugative interaction of the σ electron of ($S_1–C_2$) distribute to σ*($S_1–C_5$), N_3-C_4, $C_4–H_7$, $C_5–H_8$, and N_6-$H_{10}$of the ring. On the other hand, sides the π ($C_2–N_3$) in the ring conjugate to the anti-bonding orbital of π*($C_4–C_5$) which leads to strong delocalization of 30.49 kJ/mol. The π ($C_4–C_5$) bond is interacting with π* ($C_2–N_3$) with the energy 11.22 kcal/mol for 2-AT. The σ ($C_2–N_6$) bond is contributing energy by 1.14 kcal/mol with σ*($C_2–N_3$). In reverse trend, the σ ($C_2–N_3$) bond is contributing energy by 1.73 kcal/mol with σ* ($C_2–N_6$).

Molecular electrostatic potential analysis (MESP)

In the present study, the electrostatic potential (ESP), total electron density (ED), molecular electrostatic potential (MEP) and contour map for 2AT illustrated in Figure 11. The MEP which is a plot of electrostatic potential mapped into the constant electron density surface. The MEP is a useful property to study reactivity given that an approaching electrophile will be attracted to negative regions. In the majority of the MEP, while the maximum negative region which preferred site for electrophilic attack indications as red color, the maximum positive region which preferred site for nucleophilic attack symptoms as blue color. The importance of MEP lies in the fact that it simultaneously displays molecular size, shape as well as positive, negative and neutral electrostatic potential regions in terms of color grading (Figure 11) and is very useful in research of molecular structure with its physiochemical property relationship [37,38].

The resulting surface simultaneously displays molecular size, shape and electrostatic potential value. The colour scheme for the MESP surface is red1, electron rich, partially negative charge; blue, electron deficient, partially positive charge; light blue, slightly electron deficient region; yellow, slightly electron rich region; green, neutral; respectively. Figure.5.9 indicates that the region around nitrogen (N3) atoms represents the most negative potential region (red).The dark blue colour represents the most positive potential around the amino group region (NH2). The predominance of light green region in the MESP surfaces corresponds to a potential halfway between the two extremes red and dark blue colour.

Conclusion

The FT-IR and FT-Raman spectral measurements have been made for the 2-AT. The complete vibrational analysis and second order NBO analysis, HOMO and LUMO analysis, thermodynamic properties of the title compound was performed on the basis of DFT and HF calculations at the HF or B3LYP/6-311++G(d,p) basis set. The consistency between the calculated and experimental FT-IR and FT-Raman data indicates that the B3LYP/6-311++G(d,p) method can generates reliable geometry and related properties of the title compound.

References

[1] Brandt. A, M. Cerquetti, Corsi .G.B, Pascucci.G, Simeoni .A, Martelli .P, Valcavill .U, J. Med. Chem. 30 (1987) 764–767;
[2] Noble .S, Balfour .J.A, Drugs 51 (1996) 424–430;
[3] Ryabinina .V.A, Sinyakova .A.N, Soultraitb .V.R., Caumontb .A, Parissib .V, Zakharovac .O.D, Vasyutinac .E.L, Yurchenkoc .E, Bayandinc. R., Litvakb .S, Tarrago-Litvakb.L, Nevinskyc .G.A, Eur. J. Med. Chem. 35 (2000) 989–1000;
[4] Anderson.V.R, Curran. M.P, Drugs 67 (2007) 1947–1967;
[5] Turcotte S, Chan. D.A, Sutphin .P.D, Hay. M.P, Denny. W.A, A.J. Giaccia, Cancer Cell 2008,14,90–102;
[6] Getlik. M, Grutter. C, Simard. Kluter. J.R, Rabiller .S, Rode M. , Robubi. H.B, Rauh. A.D, J. Med. Chem. 52 (2009) 3915–3926.
[7] Isanbor C, O'Hagan D, J. Fluorine Chem. 127 (2006) 303–309
[8] Gill PMW, Johnson BG, Pople JA, Frisch MJ, Chem. Phys. Lett. 197 (1992) 499–505
[9] **Gaussian 09 Program**, Revision C.01, Frisch J, Trucks G.W, Schlegel HB, Scuseria GE, Robb MA, Cheeseman JR, Scalmani G, Barone V, Mennucci B, Petersson A, Nakatsuji H, Caricato M, Li X, Hratchian HP, Izmaylov AF, Bloino J, Zheng G, Sonnenberg JL, Hada M, Ehara M, K. Toyota K, Fukuda R, Hasegawa J, Ishida M, Nakajima T, Honda Y, Kitao O, Nakai O, Vreven T, Montgomery JA, Peralta JE, Ogliaro F, Bearpark M, Heyd JJ, Brothers E, Kudin KN, Staroverov VN, Keith T, Kobayashi R, Normand J, Raghavachari K, Rendell A, Burant JC, Iyengar SS, Tomasi J, Cossi M, Rega N, Millam JM, M. Klene M, Knox JE, Cross JB, Bakken V, Adamo C, Jaramillo J, Gomperts R, Stratmann RE, Yazyev O, Austin AJ, Cammi R, Pomelli C, Ochterski JW, Martin RL, Morokuma K, Zakrzewski G, Voth GA, Salvador P, Dannenberg JJ, Dapprich S, Daniels AD, Farkas O, Foresman JB, Ortiz JV, Cioslowski J, and Fox DJ, **Gaussian, Inc., Wallingford CT, 2010.**
[10] Becke AD, J. Chem. Phys. 98 (1993) 5648–5652.
[11] Badawi HM, Forner W, Oloriegbe YS, J. Mol. Struct. (Theochem.) 548 (2001) 219–227.
[12] Mahadevan D, Periandy S, Ramalingam S, Spectrochimica Acta Part A 79 (2011) 962– 969
[13] Batley M, Bramley R, Robinson R, Proc. R. Soc. Lond. A 369 (1979) 175–185.
[14] Zhang. R, Dub. B., Sun. G, Sun. Y, Spectrochim. Acta A 75 (2010) 1115–1124**.**
[15] Fleming I, Frontier Orbitals, Organic Chemical Reactions, Wiley, London, 1976.
[16] Asiri AM, Karabacak M, Kurt M, Alamry KA, Spectrochim. Acta A 82 (2011) 444–455.
[17] Kosar. B,Albayrak. C, Spectrochim. Acta A 78 (2011) 160–167.
[18] Socrates.G, Infrared and Raman Characteristic Group Frequencies—Tables and Charts, 3rd ed., Wiley, New York, 2001.
[19]. George. W.O, Mcintyre. P.S, Infrared Spectroscopy, John Wiley & Sons, London, 1987.
[20] Sundaraganesan. N, Saleem. H, Mohan. S, Ramalingam. M, Sethuraman.V, Spectrochimica Acta A 62 (2005) 740–751.
[21] Kumar VK, Xavier RJ, Indian J. Pure Appl. Phys. 41 (2003) 597–602.
[22] Kumar. V.K, Prabavathi. N, Spectrochimica Acta A 71 (2008) 449–457.
[23] Altun. A, Golcuk. K, Kumru. M, Journal of Molecular Structure (Theochem) 637 (2003) 155–160.
[24] Singh. S.J, Pandey S.M, Indian Journal of Pure and Applied Physics 12 (1974) 300–304.

[25] Parimalaa.K, Balachandranb.V, Journal of Spectrochimica Acta Part A 81 (2011) 711– 723
[26] Taylor. W.J, Pitzer. K.S, Journal of Research of the National Bureau of Standards 38 (1947) 1.
[27] Varsanyi. G, Assignments for vibrational spectra of seven hundred benzene derivatives, vol. 1, Wiley, New York, 1974.
[28] Gunasekaran. S, Ponnambalam. S, Muthu. S, Mariappan. L, Asian J. Phys. 16 (1) (2003) 51–63.
[29] Usha Rani. A, Sundaraganesan. N, Kurt. M, Cinar. M, Karabacak. M, Spectrochim. Acta A 75 (2010) 1523–1529.
[30] Karabacak. M, Kurt. M, Cınar. M, Coruh. A, Mol. Phys. 107 (2009) 253–264.
[31] Karabacak. M, Cinar. M, Unal. Z, Kurt. M, J. Mol. Struct. 982 (2010) 22–27.
[32] Wang. Y, Saebar. S, Pittman. C.U, J. Mol. Struct.: Theochem. 281 (1993) 9l–98l.
[33] Altun. A, Golcuk. K, Kumru. M, J. Mol. Struct.: Theochem. 637 (2003) 155–169.
[34] Arjunan. V, Mohan. S, Balamourougane. P.S, Mohan. S, Spectrochim. Acta 74A (2009) 1215–1223.
[35] James. C, AmalRaj. A, Reghunathan. R, Hubert Joe. I, JayaKumar. V.S, J. Raman Spectroscopy. 37 (2006) 1381–1392.
[36] Na. L.J, Rang. C.Z, Fang. Y.S, Zhejiang. J, Univ. Sci. 6B (2005) 584–589.
[37] Murray. J.S, Sen. K, Molecular Electrostatic Potentials, Concepts and 399 Applications, Elsevier, Amsterdam, 1996.
[38]Scrocco. E, Tomasi. J, Lowdin. P (Ed.), Advances in Quantum Chemistry, Academic Press, New York, 1978. 402.